Nat. Hazards Earth Syst. Sci. Discuss., 3, 6757–6789, 2015
www.nat-hazards-earth-syst-sci-discuss.net/3/6757/2015/
doi:10.5194/nhessd-3-6757-2015

Natural Hazards and Earth System Sciences
Discussions

Exploration of diffusion kernel density estimation in agricultural drought risk analysis: a case study in Shandong, China

W. Chen, Z. Shao, and L. K. Tiong

School of Civil Environmental Engineering, Nanyang Technological University, Singapore, Singapore

Received: 10 September 2015 – Accepted: 21 September 2015 – Published: 4 November 2015

Correspondence to: C. Wen (wchen2@e.ntu.edu.sg)

Published by Copernicus Publications on behalf of the European Geosciences Union.

Abstract

Drought caused the most widespread damage in China, making up over 50 % of the total affected area nationwide in recent decades. In the paper, a Standardized Precipitation Index-based (SPI-based) drought risk study is conducted using historical rainfall data of 19 weather stations in Shandong province, China. Kernel density based method is adopted to carry out the risk analysis. Comparison between the bivariate Gaussian kernel density estimation (GKDE) and diffusion kernel density estimation (DKDE) are carried out to analyze the effect of drought intensity and drought duration. The results show that DKDE is relatively more accurate without boundary-leakage. Combined with the GIS technique, the drought risk is presented which reveals the spatial and temporal variation of agricultural droughts for corn in Shandong. The estimation provides a different way to study the occurrence frequency and severity of drought risk from multiple perspectives.

1 Introduction

The resilience of rural households is challenged by the uncertainties of climate risks (Barnett and Mahul, 2007; Hellmuth et al., 2009; Nieto et al., 2010; Trærup, 2012). Among all the natural disasters, drought influences agriculture production the most due to its long duration and high frequency (Li et al., 2015). The IPCC fifth report (Field et al., 2014) has shown that the drought-prone regions will be exposed to severer drought risks as the regional-to-global soil–moisture ratio will continue to decrease. In China, more than two million people have been plunged back to poverty with impact of the drought in southwest China (Sivakumar, 2010).

The drought is defined as a condition of moisture deficit (e.g. of precipitation, streamflow, soil moisture) in a specific time period (Kao and Govindaraju, 2009; McKee et al., 1993). The commonly used indicators for assessing the drought includes Standardized Precipitation Index (SPI) (McKee et al., 1995), Palmer Drought Severity

NHESSD
3, 6757–6789, 2015

Index (PDSI) (Palmer, 1965) and Vegetation Condition Index (VCI) (Kogan, 1995), etc. Among the indices, SPI shows a better performance in aspects of flexibility in time scale and geography (Alley, 1984; Guttman, 1998; Heim Jr., 2002; Mishra and Singh, 2010). To further increase the effectiveness of drought risk assessment, recent studies tend to analyse drought from multivariate aspects (Michele et al., 2013), which leads to the estimation the multivariate probability density functions (PDFs) by parametric and non-parametric methods (Santhosh and Srinivas, 2013). As pointed out by Santhosh and Srinivas (2013), non-parametric PDF estimation is more reliable for analyzing hydrological risk, while parametric models are recommended when the probability density of the underlying variable is known.

Of the various ways to estimate the PDF using non-parametric functions, kernel density estimation has gained the most recognition (Santhosh and Srinivas, 2013). It has been widely adopted in the frequency analysis of flood and drought (Dalezios et al., 2000; Kannan and Ghosh, 2013; Kim et al., 2006; Moon et al., 2010; Parviz et al., 2013). Among the different kernel density estimation methods, the standardized kernel function (e.g. Gaussian kernel density estimation (GKDE)) is known for its relatively straightforward computation scheme. However, one of the disadvantages for GKDE is the boundary leakage problem that may generate biased PDF for the case of large bandwidth or left skewed variable (Santhosh and Srinivas, 2013). Another concern is the bandwidth selection which can dramatically change the shape of the estimated PDF (Kannan and Ghosh, 2013). To overcome these, an alternative – the diffusion-based kernel density estimation (DKDE), has been proposed by Botev (2010). It is shown that the DKDE performs better compared to GKDE in the aspects of improving asymptotic bias, reducing computational cost and avoiding the boundary leakage problem for left-skewed variables (e.g. precipitation) (Botev et al., 2010; Ramsey, 2014; Santhosh and Srinivas, 2013).

In the study, a SPI-based drought risk analysis is carried out using historical rainfall data of 19 weather stations from 1951 to 2006 in Shandong province, China. In the analysis, both the bivariate GKDE and DKDE are used. The occurrence frequency and

NHESSD
3, 6757–6789, 2015

severity of drought risk per growth phase are derived by both methods. Comparison between the two density estimators is discussed based on the obtained results.

2 Data

2.1 Study area

Shandong province is a part of the Northern China Plain located in the region between longitudes 34–38° N and latitudes 114–122° E (Fig. 1). It has a flat topography and a suitable climate which make it the third largest grain-producing province in China, with a 10 % contribution to the national grain production in 2012 (Yearbook, 2013).

In despite of its reputation in grain production, the province is also known as one of the most drought prone regions in China. Xue (2004) identified drought as the key peril for crop production in Shandong. It is confirmed by analyzing the area with over 30 % yield loss at province level due to five key perils (drought, flood, frost, typhoon, and hail). The result shows that 64 % of the affected area was hit by drought over the period 1978–2011 in Shandong (Yearbook, 1979–2012) (Fig. 2).

2.2 Data preparation

In this study, daily precipitation of 19 weather stations from 1951 to 2006 is collected from National Meteorological Information Center (NMIC) is compiled in Table 1. The Thiessen Polygons (Thiessen, 1911) is introduced to cover the entire Shandong province by the 19 weather stations which served as seed points (Fig. 1).

Corn is the predominant crop normally planted in June and harvested in September (Fig. 3). Growth periods is phenologically divided into Emergence (Phase I: 6–13 June), Jointing (Phase II: 14–15 July), Anthesis (Phase III: 16 July–1 August), Grain Filling (Phase IV: 2–22 August) and Maturity (23 August–13 September) (Fig. 3). Due to the importance of pre-sowing soil moisture for germination, the farmers assess the soil moisture before planting. Excessive rainfall in Phase I affects the germination and

NHESSD
3, 6757–6789, 2015

emergence rate of corn, hence hindering the development of root system and cause the corn more vulnerable to drought in the following growth phases (Kranz et al., 2008). As a result, including Phase I introduces negative correlation between the drought index and the corn yield, which affects the accuracy and does not realistically reflect the drought exposure. Therefore, Phase I is not considered in the study.

3 Methodology

For this study, the following approach is adopted to construct the SPI-based drought risk for corn in Shandong province: (i) data cleansing and detrending. Historical daily rainfall data of 19 weather stations in Shandong province are firstly cleansed and detrended for the calculation of the cumulative rainfall per growth phase, and then interpolated using Thiessen Polygons by the location of weather stations, (ii) SPI-based drought variables analysis. The SPI per growth stage of corn is developed for each region and converted into the drought duration, severity and intensity, (iii) univariate and bivariate PDFs of SPI drought variables estimation. The occurrence frequency and severity of drought risk per growth phase from multiple perspectives are conducted using DKDE and GKDE methods, (iv) joint return period analysis. The bivariate exceeding probability function is derived from the bivariate cumulative probability functions (CPFs) by integrating estimated PDFs constructed by DKDE and GKDE. By using the GIS spatial analysis tool, the spatial distribution of drought risk return periods at different drought intensities and drought durations are shown for the study region.

3.1 Data cleansing and detrending

Meteorological data may contain trends caused by artificial influence such as relocation of weather station (Hartell et al., 2006). In this study, the historical rainfall records of stations 57 415/57 465/54 830/54 909 were relocated in the 1990s. Therefore,

NHESSD
3, 6757–6789, 2015

detrending is conducted to remove the relocation-caused trend in prior to risk analysis. The conclusive changes (e.g. increasing trending caused by relocation) in rainfall will be identified with statistical regression to show the actual structural trend (e.g. fluctuation of rainfall amount) (Hartell et al., 2006). The rainfall data is assumed to be stationary in a long time span. The linear detrending method (Hartell et al., 2006) is adopted to decompose the rainfall data set $r(t)$ into linear function part and noise $\varepsilon(t)$ to test the statistical significant trend with student's t test (Eq. 1). The noise is assumed to be normally distributed with zero mean and standard deviation of σ.

$$r(t) = m_0 + m_1 t + \epsilon(t), \quad (1)$$

where m_0 and m_1 are intercept and slope of the linear trend line, respectively. By comparing the values for R^2 and the statistical significance of slope m_1 at a given confidence level under the hypothesis that m_1 is zero, the detrended rainfall can be obtained with the following function:

$$r^*(t) = \epsilon(t) + R(t_n), \quad (2)$$

where $r^*(t)$ is the detrended rainfall; $R(t_n)$, the data of most recent yield.

Following the method described in this section, the precipitation data for each of the 19 weather stations from year 1951 to year 2006 are cleansed and detrended. In the next section, the detrended rainfall will be used to compute the SPI.

3.2 Standardized Precipitation Index (SPI)

The Standardized Precipitation Index (SPI) has been chosen to model the drought events considering its flexibility in time scale and tolerance in data geographical coverage. The calculation of the SPI is based on the probability density estimation of rainfall in a given time period. Theoretically, at least 30 years of continuous precipitation data is required for the calculation (McKee et al., 1993).

Firstly, the accumulated rainfall over a chosen period of time for each insured area is fitted with a Gamma distribution (Eqs. 3 and 4) (McKee et al., 1993). The shape and

NHESSD
3, 6757–6789, 2015

scale parameters are estimated by Maximum Likelihood Estimation (Akaike, 1998). In this study, the length of each phenological corn growth stages is chosen to be the time interval (Fig. 3).

$$g(x) = \frac{1}{\beta^{\alpha}\Gamma(\alpha)} x^{\alpha-1} e^{-x/\beta}, \quad (3)$$

$$\Gamma(\alpha) = \int_0^{\infty} y^{\alpha-1} e^{-y} \mathrm{d}y, \quad (4)$$

where,

$\alpha > 0$, shape parameter;

$\beta > 0$, β scale parameter;

$x > 0$, cumulative rainfall per time scale interval;

$\Gamma(\alpha)$: the Gamma cumulative function.

Secondly, due to the difference of rainfall pattern in each region, the Gamma cumulative distribution has different values of mean and standard deviation. The variation will result in different drought characteristics. Hence, the magnitude of drought events is incomparable across different regions. In order to compare the drought severity across different regions, the Gamma cumulative distribution function is transformed to the standardized Normal cumulative distribution function with mean zero and standard deviation of unity (Eq. 5) (Guttman, 1999; Sadat Noori et al., 2012). A positive SPI indicates that rainfall amount is higher than mean value, while negative value indicates the opposite. Since the resulting SPI is independent from geographical and topographical difference (Manatsa et al., 2010), it can be used to compare the magnitude of drought events across different regions.

$$\mathrm{SPI} = \frac{(x - \hat{\mu})}{\hat{\sigma}}, \quad (5)$$

NHESSD
3, 6757–6789, 2015

where $\hat{\mu}$ represents the sample estimate of the population mean; $\hat{\sigma}$ is the sample estimate of the population standard deviation.

Theoretically, the SPI represents how much the observed precipitation data departs from the mean with regards to Gamma density function. The degree of the departure has been quantified and expressed as the SPI representing numbers of standard deviation from mean in normal distribution. For example, the cumulative probability of one negative standard deviation (SPI = −1) is 0.159 and two (SPI = −2) is 0.023. Table 2 illustrates a dry spell expressed in SPI, in which a SPI ≤ −2 is extremely dry, a SPI between −2 to −1.5 is severely dry, a SPI between −1.5 to −1 is moderately dry and a SPI between −1 to 0 is nearly normal (McKee et al., 1993).

The theory of *runs* proposed by Yevjevich (1967) has been widely used in hydrology studies (Dalezios et al., 2000; Kim et al., 2006; Mishra and Singh, 2009; Shiau et al., 2007), which identifies drought risk in a continuous period by setting a truncation level of moisture. Figure 4 explains the SPI-based drought risk parameters including drought duration D, intensity I and severity S:

- The drought duration D is the period when the SPI is below a prescribed truncation level. The effect of drought on crop yield is an accumulative process. Hence the occurrence of normal rainfall ($-1 < \mathrm{SPI} < 0$) at some points of the crop growth period, does not change the fact that the accumulated shortage of rainfall during the same period has already demonstrated occurrence of drought. It is shown in the Fig. 4 due to the accumulated rainfall shortage at each growth period, the crop yield is affected. Therefore the SPI = 0 is marked as the truncation level.

- Drought severity S is the negative sum of the SPI in drought duration D as follows:

$$S = -\sum_{1}^{D} \mathrm{SPI}_i. \tag{6}$$

NHESSD
3, 6757–6789, 2015

– The drought intensity I is the average SPI below the truncation during the drought duration D, calculated by dividing the drought severity S by the drought duration D.

3.3 Gaussian kernel density and diffusion kernel density

To quantify the drought risk during a corn growth period, both drought duration and intensity are analysed using the DKDE and GKDE estimators. The K-S test is used to estimate the effectiveness of the two. This section provides a brief introduction of GKDE and DEKE.

3.3.1 Gaussian kernel density estimation

Kernel density estimation is firstly introduced by Rosenblatt (1956) and the general form is given by Härdle (1991). Let $(x_1 x_2, \ldots, x_n)$ denote the random variables, the bivariate density function is given by:

$$\hat{f}(x,h) = \frac{1}{nh_1h_2}\sum_{i=1}^{n} K\left(\frac{x_1 - x_{i1}}{h_1}\right) K\left(\frac{x_2 - x_{i2}}{h_2}\right), \quad (7)$$

where, h_1 and h_2 are the bandwidths for the two variables (x_{i1}, x_{i2}); n indicates the number of observations. The K represents the Gaussian kernel function and $K = (2\pi)^{-1/2} e^{-(t^2)/2}$.

The bandwidth is determined under the assumption that the underlying true density is normally distributed and targets to minimize the asymptotic mean integrated square error (AMISE) between the kernel density and the target density (Silverman, 1986). When the Gaussian function is adopted in multivariate case, the optimal bandwidth h_d at d_{th} dimension with GKDE is given by:

$$h_d = \left[\frac{4}{n(p+2)}\right]^{\frac{1}{p+4}} \sigma_d, \quad (8)$$

NHESSD
3, 6757–6789, 2015

where p is the number of dimension and σ_d, the standard deviation in dimension d.

3.3.2 Bivariate diffusion kernel density estimation

The rescaled SPI-based variables, duration and intensity, are denoted by $x = (x_1, x_2, \ldots, x_n)$ and $y = (y_1, y_2, \ldots, y_n)$ respectively. The bivariate histogram of x and y is converted by discrete cosine transform and bivariate diffusion kernel density function is given as:

$$\hat{f}(x,y) = \sum_{i=1}^{m}\sum_{j=1}^{m} \frac{1}{2\sqrt{t_x t_y}} e^{-\left(\frac{(x-x_i)^2}{2t_x} + \frac{(y-y_i)^2}{2t_y}\right)}. \quad (9)$$

An improved plug-in bandwidth selection method is introduced by Botev (2010) with parameter $\hat{t}^*$ given by:

$$\hat{t}^* = (2\pi n(\psi_{0,2} + \psi_{2,0} + 2\psi_{1,1}))^{-1/3}, \quad (10)$$

where $\psi_{i,j}$ is digamma function of order i through j evaluate by $\hat{t}_{i,j}$:

$$\psi_{i,j} = (-1)^{i+j} \int \left(\frac{\delta^{i+j}}{\delta x^i \delta y^j} f(x)\right)^2 \mathrm{d}x, \quad (11)$$

$$\hat{f}_{i,j} = \left(\frac{1 + 2^{-i-j-1}}{3} \frac{2q(i)q(j)}{n\left(\hat{\psi}_{i+1,j} + \hat{\psi}_{i,j+1}\right)}\right)^{1/(2+i+i)}, \quad (12)$$

NHESSD
3, 6757–6789, 2015

where

$$q(l) = \begin{cases} (-1)^{l} \frac{1\times3\times5\times\ldots\times(2l-1)}{\sqrt{2\pi}}, & l \geq 1 \\ \frac{1}{\sqrt{2\pi}}, & l = 0, \end{cases} \tag{13}$$

$$t_x = \left(\frac{\hat{\psi}_{0,2}^{3/4}}{4\pi N \hat{\psi}_{0,2}^{3/4} \left(\hat{\psi}_{1,1} + \sqrt{\hat{\psi}_{2,0}\hat{\psi}_{0,2}} \right)} \right)^{1/3}, \tag{14}$$

$$t_y = \left(\frac{\hat{\psi}_{2,0}^{3/4}}{4\pi N \hat{\psi}_{0,2}^{3/4} \left(\hat{\psi}_{1,1} + \sqrt{\hat{\psi}_{2,0}\hat{\psi}_{0,2}} \right)} \right)^{1/3}. \tag{15}$$

The estimation of t_x and t_y is based on the iteration procedure: compare the difference between $\hat{t}^*$ and $\hat{t}_{i,j}$, if $\hat{t}^* < \hat{t}_{i,j}$, then t_x and t_y are calculated by Eqs. (14) and (15). Otherwise, $\hat{t}_{i,j}$ is updated to $\hat{t}^*$ and the previous steps are iterated until $\hat{t}^* = \hat{t}_{i,j}$.

3.4 Return period analysis

After the estimation of the joint PDFs of the duration and intensity, the joint return period is calculated from the bivariate cumulative probability functions (CPFs) by aggregating the joint PDFs for different drought events. The return period R is defined as the average time recurrence interval that a certain magnitude of event has the probability $1/R$ of being exceeded. The bivariate return period can be defined by (Li et al., 2013):

$$R_{x,y} = \frac{1}{P(X \geq x_i \text{ or } Y \geq y_i)} = \frac{1}{1 - K(F_X(x), F_y(y))}, \tag{16}$$

NHESSD
3, 6757–6789, 2015

where $F(xy)$ represents the joint cumulative density function of variable x and y; $K(\cdot)$ is the diffusion kernel function.

4 Result and discussion

To examine the performance of the DKDE and GKDE, both methods are applied to SPI per growth phase of the19 weather stations in Shandong province. The data from Weather station 57 414 is taken as an example. The joint return period of drought duration and drought intensity based on the DKDE is developed for the spatial drought risk analysis in Shandong province. The performance of the DKDE and GKDE is examined by comparing the SPI-based corn drought risk for all the four growth phases in two aspects: drought duration and drought intensity.

4.1 Standardized Precipitation Index

The monthly SPI per year and SPI of Phase II to V of each weather station are separately calculated and plotted in Fig. 5. The fluctuation of SPI per growth phase from 1951 to 2006 indicates that the lowest SPI is around −2 in the last 56 years. More drought events occur in Phase III and IV, corresponding to the Anthesis and Grain Filling phases. Lots of experiments and literatures have shown that the Anthesis and Grain Filling phases are the most water-sensitive phases in the corn growth cycle (Allen et al., 1998). It also indicates that the frequency of drought increases in the recent 20 years, especially in Phase II and III.

4.2 Univariate and bivariate probability density function analysis

Figure 6 shows the bivariate PDF of drought intensity and duration for Phases II–V estimated by DKDE and GKDE separately. One thing can be observed from the figure is that the DKDE performances better than the GKDE in terms of the boundary leakage or boundary bias problem. For example, Fig. 6b shows that the PDF estimated by GKDE

NHESSD
3, 6757–6789, 2015

results in negative drought intensity, and the left boundary of GKDE marginal PDF estimation extends into the negative region of drought intensity in Fig. 6c. Furthermore, the K-S test at 95 % confidence level is shown in Table 3. It indicates that DKDE has a better goodness of fit for univariate PDF for drought intensity compared to the one using GKDE. It is shown that 92 % of the p values of K-S test estimated for DKDE are higher than those estimated from GKDE. An overall of 76 drought intensity samples based on SPI for each growth phase and 19 samples for the whole growth period are tested. The 19 samples based on SPI of each month in the data available years in each station are tested as well. For GKDE, 19 out of 114 samples are rejected by the hypothesis that the drought intensity follows the specified distribution and only 6 are rejected by the hypothesis using DKDE. Hence, the DKDE is considered as a better candidate for the bivariate PDF analysis of drought risk in the next step.

4.3 Return period analysis

The bivariate exceeding probability is shown in Fig. 7. It is later used to obtain the joint return period of drought duration and drought intensity. Comparison of the joint return period estimated by DKDE and GKDE is shown in Fig. 8. The figure indicates that the drought intensity estimated by GKDE is higher than that of DKDE given the same drought duration and vice versa. Figure 9 shows the joint return period of drought duration and intensity in Phases II, III, IV and V estimated by DKDE for weather station 57 414.

The joint return period by DKDE for Shandong Province is computed under the condition of 1 year drought duration and drought intensity 2 (SPI = −2). The spatial distribution of the joint return period for the combined growth phases and Phases II–V in Shandong are shown separately in Figs. 10 and 11. A higher return period characterized by the given drought duration and drought intensity can be observed in the central region of the province, indicating a lower drought risk in this area compared to the rest. The return period is lower in the northeast and southeast of the

NHESSD
3, 6757–6789, 2015

province throughout all the growth phases (Phases II–V), indicating a higher drought vulnerability in these regions.

Regions around the weather station 54 936 show that the highest return period (6.7 years) of drought risk in Phase II among the 19 regions. In Phases III and IV, the average return periods of all regions are approximately 2, while region around weather station 54 936 and central region of the province show the highest return period. For Phase V, the weather station 54 836 located in the central of Shandong shows the highest return period (5.3). Overall, the spatial distribution of the joint return period for four corn growth phases in Shandong shows a higher return period in the central area and south area around weather station 54 936. A study (Wang et al., 2014) shows the same result of spatial and temporal drought risk near Taishan (central area) and Rizhao (weather station 54 936) in summer and autumn (corn growth season) with lower drought frequency from 1961 to 2008. In addition, the north, northeast and southwest regions are more exposed to extreme drought in the corn growth season, especially in phases II and IV, which are consistent with the study by Wang (2014).

5 Conclusions

Better understanding of the occurrence frequency and severity of drought risk can help financial institutions and governments to capture the potential losses and compensate the uncertainties of caused by extreme drought events. Therefore, it is necessary to conduct ample studies for the related risks beforehand.

The study provides an alternative to understand the occurrence and severity of drought risk from multiple perspectives. As shown in Sect. 4, the DKDE is more effective than GKDE in estimating the bivariate PDFs of drought risk in terms of accuracy and the ability to avoid boundary-leakage problem. Combined with GIS spatial analysis techniques, spatial and temporal variations of agricultural droughts for corn in Shandong province are revealed. It is shown that the central region is less vulnerable to drought compared to the other regions. Therefore, using the DKDE

NHESSD
3, 6757–6789, 2015

function to analyze agricultural drought will eventually help the financial institutes determine compensation by providing a reference for identifying regional drought risk vulnerability, and offer important technological support for drought management for government.

References

Akaike, H.: Information theory and an extension of the maximum likelihood principle, in: Selected Papers of Hirotugu Akaike, Springer, New York, 199–213, 1998.

Allen, R. G., Pereira, L. S., Raes, D., and Smith, M.: Crop Evapotranspiration: Guidelines for Computing Crop Water Requirements, FAO, Rome, 1998.

Alley, W. M.: The Palmer drought severity index: limitations and assumptions, J. Clim. Appl. Meteorol., 23, 1100–1109, 1984.

Barnett, B. J. and Mahul, O.: Weather index insurance for agriculture and rural areas in lower-income countries, Am. J. Agr. Econ., 89, 1241–1247, 2007.

Botev, Z., Grotowski, J., and Kroese, D.: Kernel density estimation via diffusion, Ann. Stat., 38, 2916–2957, 2010.

Dalezios, N. R., Loukas, A., Vasiliades, L., and Liakopoulos, E.: Severity-duration-frequency analysis of droughts and wet periods in Greece, Hydrolog. Sci. J., 45, 751–769, 2000.

Field, C. B., Barros, V. R., Dokken, D. J., Mach, K. J., Mastrandrea, M. D., Bilir, T. E., Chatterjee, M., Ebi, K. L., Estrada, Y. O., and Genova, R. C.: IPCC, 2014: Climate Change 2014: Impacts, Adaptation, and Vulnerability, Part A: Global and Sectoral Aspects, Contribution of Working Group II to the Fifth Assessment Report of the Intergovernmental Panel on Climate Change, Cambridge University Press, Cambridge, UK, New York, NY, USA, 2014.

Guttman, N. B.: Comparing the Palmer Drought Index and the Standardized Precipitation Index, J. Am. Water Resour. As., 34, 113–121, 1998.

Guttman, N. B.: Accepting the SPI: a calculation algorithm, J. Am. Water Resour. As., 35, 311–322, 1999.

Hartell, J., Ibarra, H., Skees, J., and Syroka, J.: Risk Managemenet in Agriculture for Natural Hazards, ISMEA, Rome, 2006

Härdle, W.: Smoothing Techniques: With Implementation in S, Springer, New York, 1991.

NHESSD
3, 6757–6789, 2015

Heim Jr., R. R.: A review of twentieth-century drought indices used in the United States, B. Am. Meteorol. Soc., 83, 1149–1165, 2002.
Hellmuth, M. E., Osgood, D. E., Hess, U., Moorhead, A., and Bhojwani, H.: Index Insurance and Climate Risk: Prospects for Development and Disaster Management, International Research Institute for Climate and Society (IRI), New York, 2009.
Kannan, S. and Ghosh, S.: A nonparametric kernel regression model for downscaling multisite daily precipitation in the Mahanadi basin, Water Resour. Res., 49, 1360–1385, 2013.
Kao, S. C. and Govindaraju, R. S.: A copula-based joint deficit index for droughts, J. Hydrol., 380, 121–134, 2009.
Kim, T. W., Valdes, J. B., and Yoo, C.: Nonparametric approach for bivariate drought characterization using Palmer drought index, J. Hydrol. Eng., 11, 134–143, 2006.
Kogan, F. N.: Droughts of the late 1980s in the United States as derived from NOAA polar-orbiting satellite data, B. Am. Meteorol. Soc., 76, 655–668, 1995.
Kranz, W. L., Irmak, S., Van Donk, S. J., Yonts, C. D., and Martin, D. L.: Irrigation Management for Corn, Neb Guide, University of Nebraska, Lincoln, 2008.
Li, N., Liu, X., Xie, W., Wu, J., and Zhang, P.: The return period analysis of natural disasters with statistical modeling of bivariate joint probability distribution, Risk Anal., 33, 134–145, 2013.
Li, Y., Gu, W., Cui, W., Chang, Z., and Xu, Y.: Exploration of copula function use in crop meteorological drought risk analysis: a case study of winter wheat in Beijing, China, Nat. Hazards, 1–15, 2015.
Manatsa, D., Mukwada, G., Siziba, E., and Chinyanganya, T.: Analysis of multidimensional aspects of agricultural droughts in Zimbabwe using the Standardized Precipitation Index (SPI), Theor. Appl. Climatol., 102, 287–305, 2010.
McKee, T. B., Doesken, N. J., and Kleist, J.: The relationship of drought frequency and duration to time scales, in: Proceedings of the 8th Conference on Applied Climatology, 17–22 January 1993, California, American Meteorological Society Boston, MA, 17, 179–183, 1993.
McKee, T. B., Doesken, N. J., and Kleist, J.: Drought monitoring with multiple time scales, in: Ninth Conference on Applied Climatology, 15–20 January 1995, Texas, American Meteorological Society, Boston, 1995.
Michele, C., Salvadori, G., Vezzoli, R., and Pecora, S.: Multivariate assessment of droughts: frequency analysis and dynamic return period, Water Resour. Res., 49, 6985–6994, 2013.

NHESSD
3, 6757–6789, 2015

Mishra, A. K. and Singh, V. P.: Analysis of drought severity-area-frequency curves using a general circulation model and scenario uncertainty, J. Geophys. Res., 114, D06120, doi:10.1029/2008JD010986, 2009.
Mishra, A. K. and Singh, V. P.: A review of drought concepts, J. Hydrol., 391, 202–216, 2010.
Moon, Y. I., Oh, T. S., Kim, M. S., and Kim, S. S.: A drought frequency analysis for Palmer Drought Severity Index using boundary kernel function, in: World Environmental and Water Resources Congress, 16–20 May 2010, Providence, Rhode Island, United States, 2708–2716, 2010.
Nieto, J. D., Cook, S. E., Laderach, P., Fisher, M. J., and Jones, P. G.: Rainfall index insurance to help smallholder farmers manage drought risk, Climate and Development, 2, 233–247, 2010.
Palmer, W. C.: Meteorological Drought, Office of Climatology, US Weather Bureau, Washington, DC, 1965.
Parviz, H. J., Akhoond-Ali, A. M., and Nazemosadat, M. J.: Nonparametric kernel estimation of annual precipitation over Iran, Theor. Appl. Climatol., 112, 193–200, 2013.
Ramsey, A. F.: An application of kernel density estimation via diffusion to group yield insurance, in: 2014 AAEA Annual Meeting, 27–29 July 2014, Minneapolis, 2077, 2014.
Rosenblatt, M.: Remarks on some nonparametric estimates of a density function, Ann. Math. Stat., 27, 832–837, 1956.
Sadat Noori, S. M., Liaghat, A. M., and Ebrahimi, K.: Prediction of crop production using drought indices at different time scales and climatic factors to manage drought risk, J. Am. Water Resour. As., 48, 1–9, 2012.
Santhosh, D. and Srinivas, V. V.: Bivariate frequency analysis of floods using a diffusion based kernel density estimator, Water Resour. Res., 49, 8328–8343, 2013.
Shiau, J. T., Feng, S., and Nadarajah, S.: Assessment of hydrological droughts for the Yellow River, China, using copulas, Hydrol. Process., 21, 2157–2163, 2007.
Silverman, B. W.: Density Estimation for Statistics and Data Analysis, CRC press, London, 1986.
Sivakumar, M. V.: Agricultural drought – WMO perspectives, in: Agricultural Drought Indices: Proceedings of an Expert Meeting, 2–4 June 2010, Murcia, Spain, 219, 2010.
Thiessen, A. H.: Precipitation averages for large areas, Mon. Weather Rev., 39, 1082–1089, 1911.

NHESSD
3, 6757–6789, 2015

Trærup, S. L. M.: Informal networks and resilience to climate change impacts: a collective approach to index insurance, Global Environ. Chang., 22, 255–267, 2012.
Wang, X. L., Hou, X. Y., Li, Z., and Wang, Y. D.: Spatial and Temporal Characteristics of Meteorological Drought in Shandong Province, China, from 1961 to 2008, Advances in Meteorology, 2014, 873593, doi:10.1155/2014/873593, 2014.
Xue, X.: Study on Quantificational Relation Between Drought and Agriculture Yield in Shandong Province, Ocean University of China, Qingdao, 2004.
Yearbook: Shandong Statistical Yearbook, China Statistics Press, Beijing, 1979–2012.
Yearbook: China Statistical Year Book 2013, China Statistics Press, Beijing, 2013.
Yevjevich, V.: Review: an objective approach to definitions and investigations of continental hydrologic droughts, Fort Collins, Colorado State University, 1967, 19 p. (Hydrology paper no. 23), J. Hydrol., 7, 353, 1967.

NHESSD
3, 6757–6789, 2015

Table 1. Locations and daily rainfall data records of 19 weather stations in Shandong province.

	Station ID	Latitude	Longitude	Remarks
1	54714/54715	37.2	116.3	Data before 1995 is collected from 57 414
2	54725	37.3	117.3	
3	54736	37.3	118.4	
4	54751	37.6	120.4	
5	54753	37.4	120.2	
6	54764/57465	37.3	121.2	Data before 1992 is collected from 54 764
7	54774	37.3	122.1	
8	54776	37.2	122.4	
9	54823	36.4	116.6	
10	54824/54830	36.5	118.0	Data before 1995 is collected from 54 824
11	54827	36.1	117.1	
12	54836	36.1	118.1	
13	54843	36.5	119.1	
14	54852	36.6	120.4	
15	54857	36.0	120.2	
16	54906/54909	35.1	115.3	Data before 1995 is collected from 54 906
17	54916	35.3	116.5	
18	54936	35.4	118.5	
19	54945	35.2	119.3	

NHESSD
3, 6757–6789, 2015

Table 2. Drought categories based on Standardized Precipitation Index.

SPI Values	Drought Categories
$SPI \leq -2$	Extremely Dry
$-2 \leq SPI \leq -1.5$	Severely Dry
$-1.5 \leq SPI \leq -1$	Moderately Dry
$-1 \leq SPI \leq 1$	Near Normal
$1 \leq SPI \leq 1.5$	Moderately Wet
$1.5 \leq SPI \leq 2$	Severely Wet
$SPI \geq 2$	Extremely Wet

NHESSD
3, 6757–6789, 2015

Table 3. *p* value of K-S test statistics for univariate PDF of drought intensity estimated by DKDE and GKDE.

	Drought Intensity											
		DKDE						GKDE				
ID	Monthly	II–IV	II	III	IV	V	Monthly	II–IV	II	III	IV	V
54 714	0.5	0.6	0.2	0.0	0.2	0.9	0.7	0.1	0.2	0.0	0.1	0.7
54 725	0.7	0.8	0.8	0.2	0.6	0.1	0.7	0.5	0.7	0.1	0.1	0.0
54 736	0.9	0.1	0.0	0.2	0.6	0.2	0.6	0.0	0.1	0.3	0.2	0.0
54 741	0.8	0.8	0.1	0.7	0.9	0.5	0.8	0.2	0.1	0.1	0.2	0.1
54 753	0.7	0.0	0.8	0.5	0.3	0.2	0.7	0.0	0.1	0.2	0.0	0.0
54 764	0.8	0.2	0.4	0.6	0.2	0.4	0.7	0.1	0.1	0.2	0.0	0.5
54 774	0.9	0.2	0.9	0.9	0.5	0.9	0.8	0.1	0.3	0.7	0.3	0.3
54 776	0.4	0.0	0.6	0.9	0.2	0.9	0.6	0.0	0.2	0.6	0.2	0.5
54 823	0.8	0.5	0.9	0.9	0.9	0.8	0.8	0.5	0.3	0.2	0.2	0.3
54 824	0.7	0.9	0.5	0.9	0.5	0.2	0.6	0.9	0.1	0.2	0.1	0.0
54 827	0.8	0.4	0.9	0.5	0.6	0.2	0.8	0.1	0.2	0.5	0.1	0.5
54 836	0.6	0.9	0.2	0.2	0.5	0.5	0.6	0.4	0.2	0.1	0.2	0.2
54 843	0.6	0.9	0.9	0.9	0.9	0.8	0.8	0.6	0.3	0.2	0.2	0.3
54 852	0.6	0.3	0.2	0.0	0.2	0.8	0.6	0.0	0.2	0.0	0.1	0.2
54 857	0.7	0.2	0.4	0.2	0.2	0.2	0.5	0.0	0.1	0.0	0.1	0.0
54 906	0.8	0.0	0.2	0.7	0.2	0.2	0.7	0.0	0.2	0.8	0.1	0.0
54 916	0.8	0.7	0.5	0.9	0.7	0.1	0.7	0.5	0.0	0.2	0.1	0.0
54 936	0.7	0.7	0.8	0.7	0.9	0.8	0.7	0.7	0.1	0.4	0.5	0.2
54 945	0.4	0.0	0.9	0.7	0.2	0.1	0.4	0.0	0.9	0.2	0.1	0.0

NHESSD
3, 6757–6789, 2015

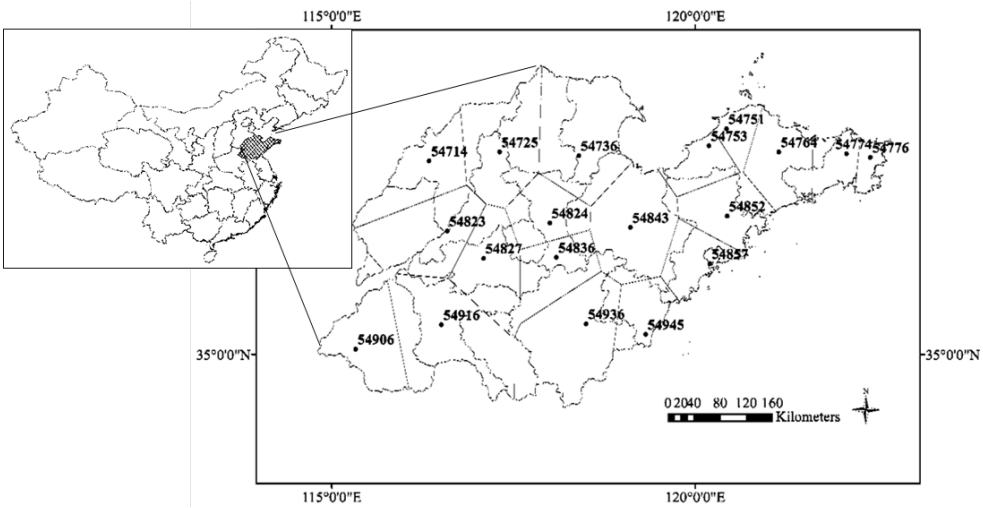

Figure 1. Location of Shandong province in China (top), Shandong province (below) with 19 weather stations (points) and Insured Areas by Thiessen polygons.

NHESSD
3, 6757–6789, 2015

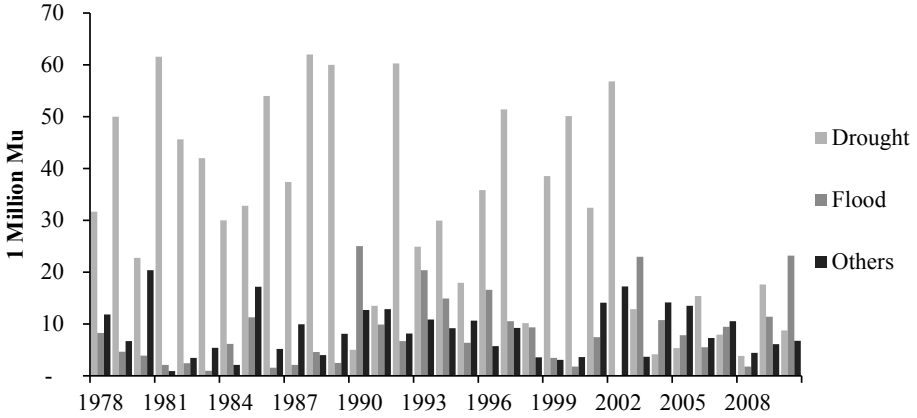

Figure 2. Sown agricultural area affected by drought, flood, and other perils in Shandong province from 1978 to 2011 (1 ha = 15 Mu).

NHESSD
3, 6757–6789, 2015

Growth Stages	Emergence	Jointing	Anthesis	Graining Filling	Maturity
Dates	6 Jun – 13 Jun	14 Jun – 15 Jul	16 Jul – 1 Aug	2 Aug – 22 Aug	23 Aug – 13 Sep
Duration	8 days	32 days	17 days	21 days	22 days

Figure 3. Corn phenological growth stages in Shandong province.

NHESSD
3, 6757–6789, 2015

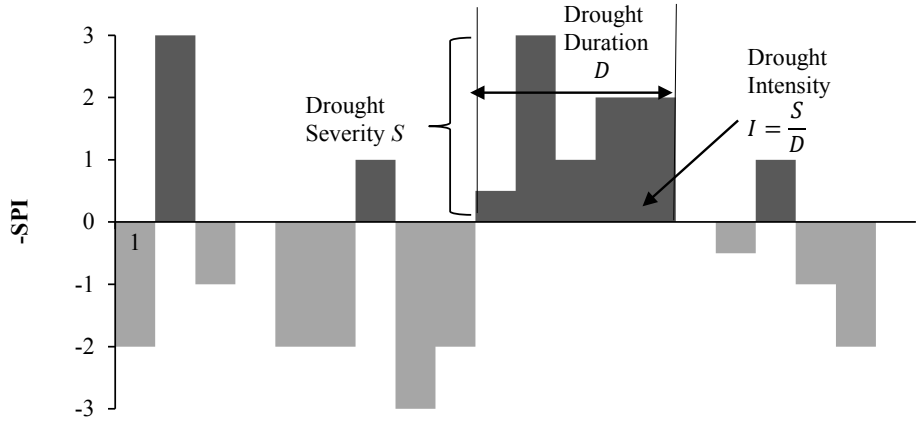

Figure 4. Standardized Precipitation Index (SPI)-based drought duration D, intensity I and severity S.

NHESSD
3, 6757–6789, 2015

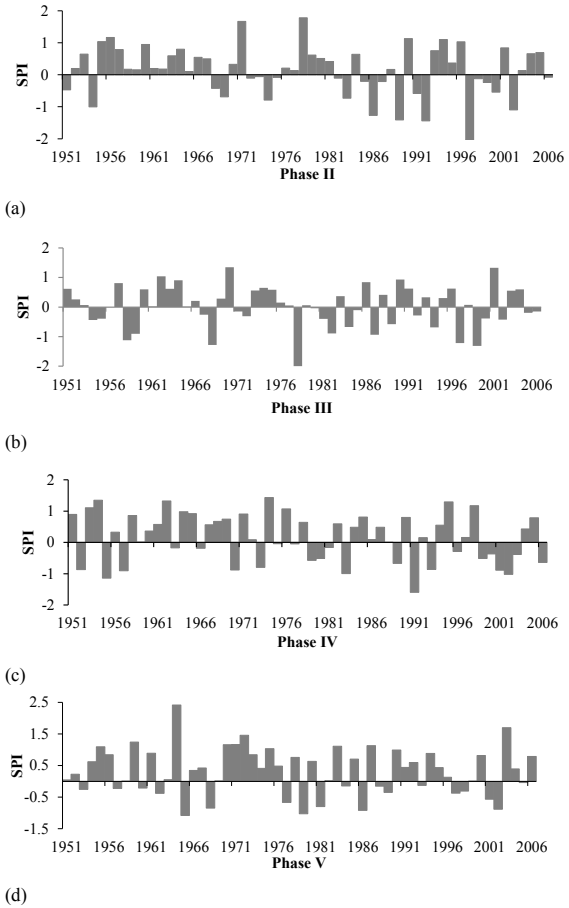

Figure 5. SPI per corn Growth Phase II **(a)**, III **(b)**, IV **(c)** and V **(d)** for Weather station 57 414, 1951–2006.

NHESSD
3, 6757–6789, 2015

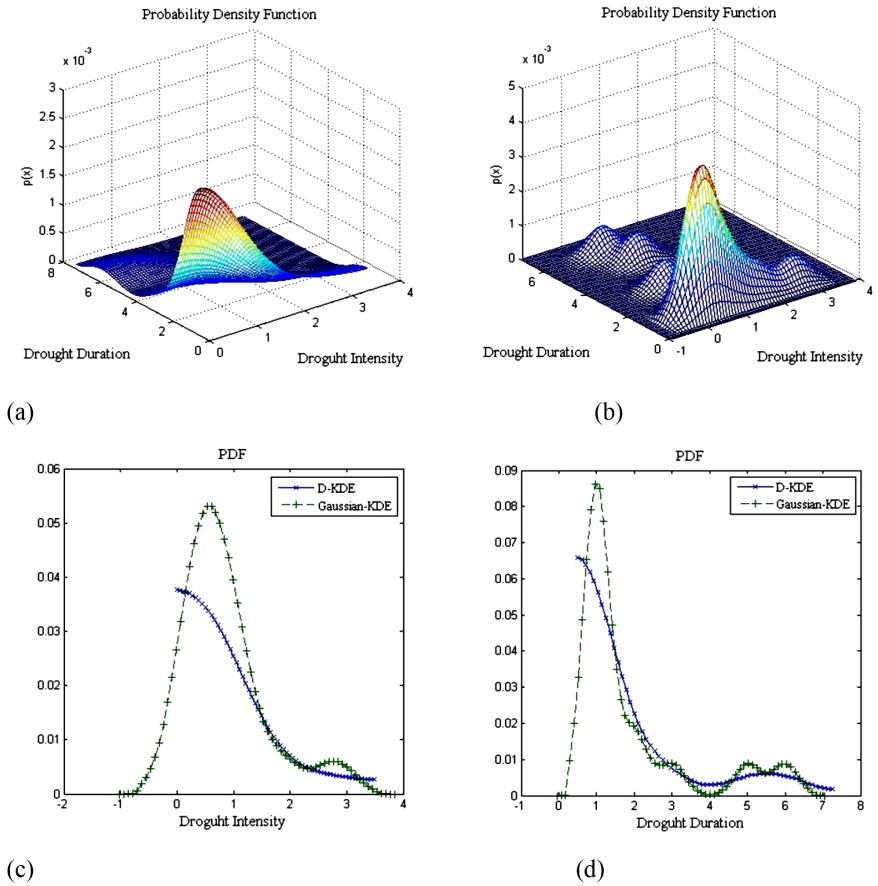

Figure 6. Weather station 54 714 **(a)** DKDE estimated bivariate PDF of SPI based drought risk (PII–PV), **(b)** GKDE estimated bivariate PDF of SPI based drought risk (PII–PV), **(c)** comparison of univariate PDF for drought intensity by DKDE and DKDE, **(d)** comparison of univariate PDF for drought duration by DKDE and GKDE.

NHESSD
3, 6757–6789, 2015

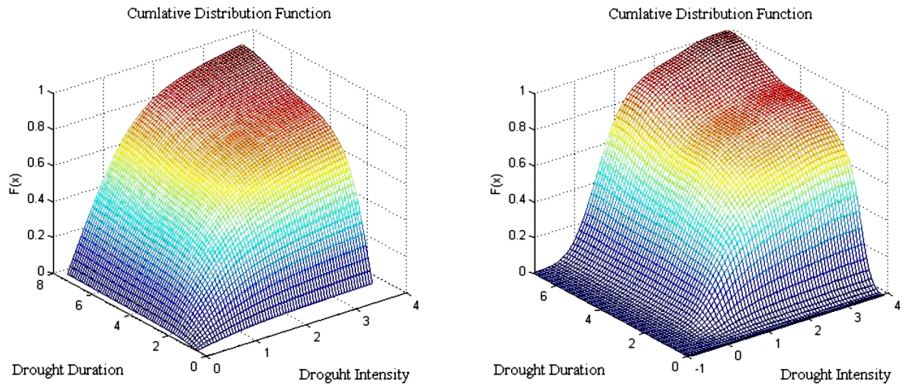

(a) (b)

Figure 7. (a) DKDE estimated bivariate CDF of SPI based drought risk (PII–PV), **(b)** GKDE estimated bivariate CDF of SPI based drought risk (PII–PV).

NHESSD
3, 6757–6789, 2015

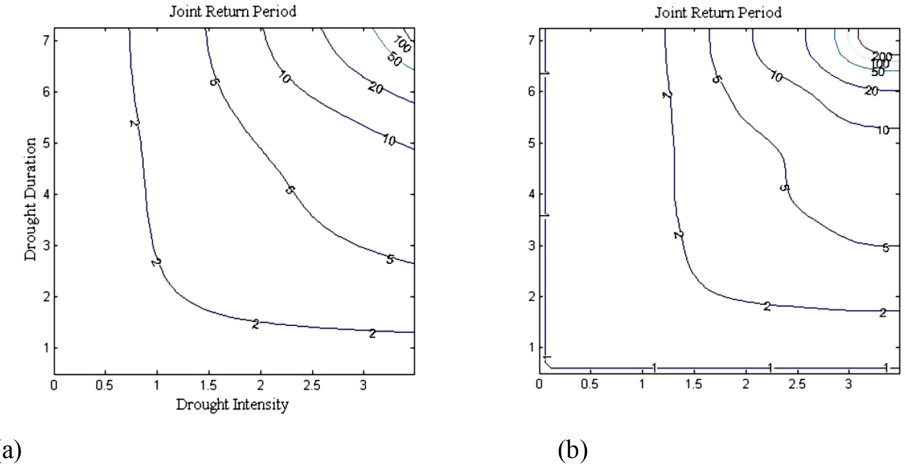

Figure 8. (a) Joint return period of drought duration and drought severity for corn (Phase II–V) estimated by DKDE. **(b)** Joint return period of drought duration and drought severity for corn (Phase II–V) estimated by GKDE (weather station 57 414).

NHESSD
3, 6757–6789, 2015

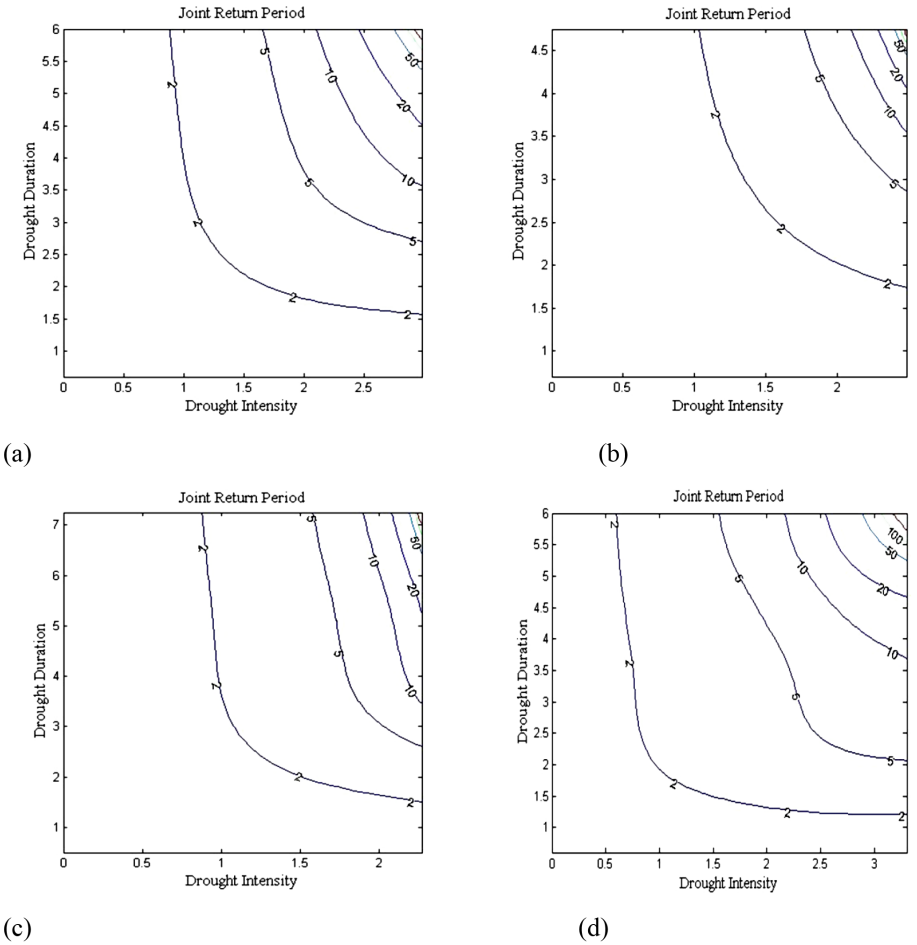

Figure 9. Joint return period of drought duration and drought severity for corn growth phase II, III, IV and V (weather station 57 414).

NHESSD
3, 6757–6789, 2015

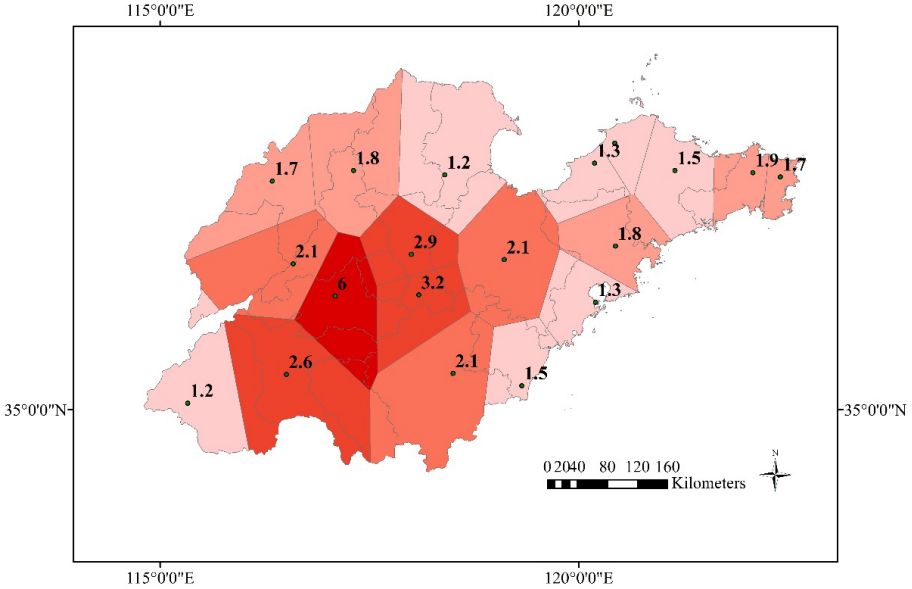

Figure 10. Map of Shandong province with joint return period with drought duration of 1 year and drought intensity of 2 for whole growth phases (Phase II–V).

NHESSD
3, 6757–6789, 2015

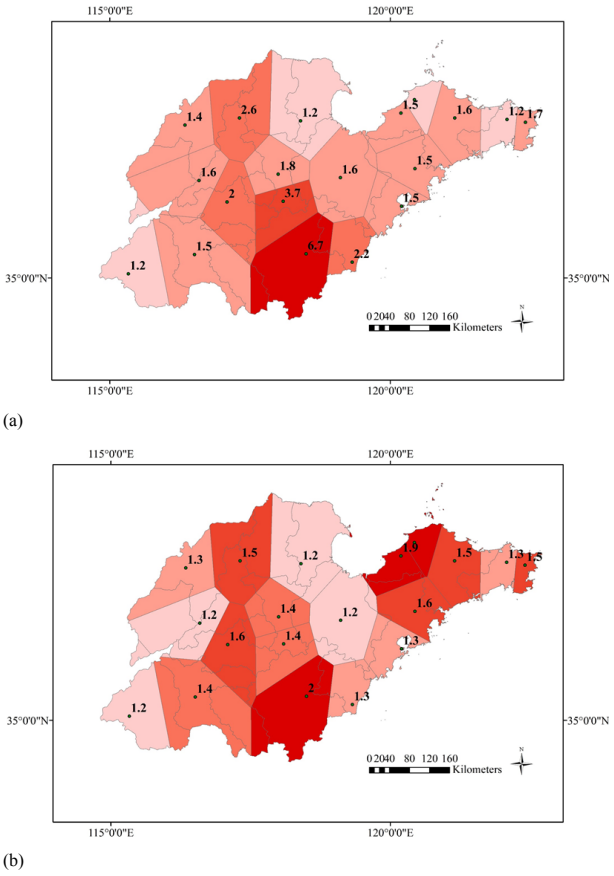

Figure 11.

NHESSD
3, 6757–6789, 2015

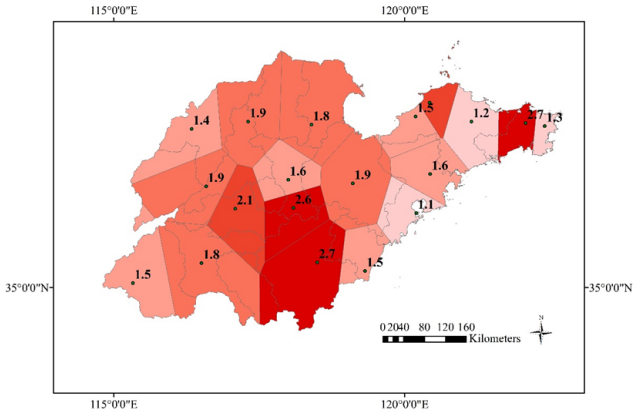

(c)

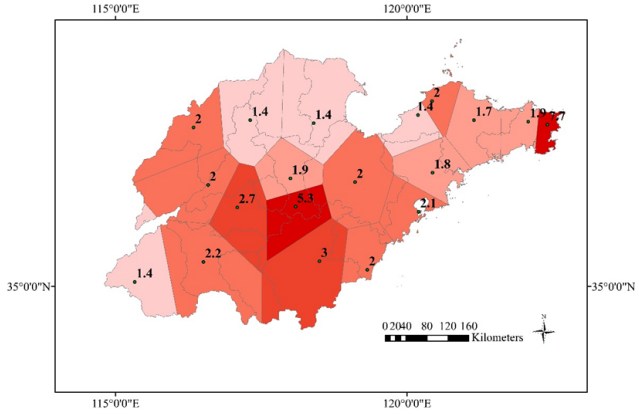

(d)

Figure 11. Map of Shandong province with joint return period with drought duration of 1 year and drought intensity of 2 **(a)** Phase II, **(b)** Phase III, **(c)** Phase IV, **(d)** Phase V.

NHESSD
3, 6757–6789, 2015